Changes in rivers inputs during the last decades significantly impacted the biogeochemistry of the eastern Mediterranean basin: A modelling study

R. Pagès, Melika Baklouti, Nicolas Barrier, C. Richon, J.-C. Dutay, T. Moutin

Changes in rivers inputs during the last decades significantly impacted the biogeochemistry of the eastern Mediterranean basin: A modelling study

R. Pagès, Melika Baklouti, N. Barrier, C. Richon, J.-C. Dutay, T. Moutin

Version of Record: https://www.sciencedirect.com/science/article/pii/S0079661119304227
Manuscript_13e320718774c726ea5cab20f5219ea3

Changes in rivers inputs during the last decades significantly impacted the biogeochemistry of the eastern Mediterranean basin: a modelling study

R. Pagès[a,*], M. Baklouti[a,*], N. Barrier[b], C. Richon[c], J-C. Dutay[d], T. Moutin[a]

[a] *Aix Marseille Université, Université de Toulon, CNRS, IRD, MIO UM 110 , 13288, Marseille, France*
[b] *MARBEC, Institut de Recherche pour le Développement (IRD), Université de Montpellier, Centre National de la Recherche Scientifique (CNRS), Ifremer, place Eugène Bataillon, Montpellier, France*
[c] *School of Environmental Sciences, University of Liverpool, Liverpool, UK*
[d] *LSCE/IPSL, Laboratoire des Sciences du Climat et de l'Environnement, CEA-CNRS-UVSQ, Gif-sur-Yvette, France*

Abstract

The Mediterranean Sea (MS) is a semi-enclosed sea characterized by a zonal west-east gradient of oligotrophy, where microbial growth is controlled by phosphate availability in most situations. External inputs of nutrients including Gibraltar inputs, river inputs and atmospheric deposition are therefore of major importance for the biogeochemistry of the MS. This has long been considered to be driven mainly by nutrient exchanges at Gibraltar. However, recent studies indicate that river inputs significantly affect nutrients concentrations in the Mediterranean Sea, although their resulting impact on its biogeochemistry remains poorly understood.

In this study, our aim was to make good this lack by addressing the large-scale and long-term impact of variations in river inputs on the biogeochemistry of the Mediterranean Sea over the last decades, using a coupled physical-biogeochemical 3D model (NEMO-MED12/Eco3M-Med).

As a first result, it has been shown by the model that the strong diminu-

*Corresponding author. Address: MIO Campus Technologique et Scientifique de Luminy 163 avenue de Luminy - Bâtiment Méditerranée 13288 Marseille cedex 09

Email addresses: remi.pages@mio.osupytheas.fr (R. Pagès), melika.baklouti@mio.osupytheas.fr (M. Baklouti)

tion (60 %) of phosphate (PO_4) in river inputs into the Mediterranean Sea since the end of the 1980s induced a significant lowering of PO_4 availability in the sub-surface layer of the Eastern Mediterranean Basin (EMB). One of the main consequences of PO_4 diminution is the rise, never previously documented, of dissolved organic carbon (DOC) concentrations in the surface layer (by 20% on average over the EMB). Another main result concerns the gradual deepening of the top of the phosphacline during the period studied, thus generating a shift between the top of the nitracline and the top of the phosphacline in the EMB. This shift has already been observed *in situ* and documented in literature, but we propose here a new explanation for its occurrence in the EMB. The last main result is the evidence of the decline in abundance and the reduction of size of copepods calculated by the model over the years 1985-2010, that could partially explain the reduction in size of anchovy and sardine recently recorded in the MS.
In this study, it is shown for the first time that the variations in river inputs that occurred in the last decades may have significantly altered the biogeochemical cycles of two key elements (P and C), in particular in the EMB. To conclude, the magnitude of the biogeochemical changes induced by river inputs and runoff alone over the last thirty years clearly calls for the use of realistic scenarios of river inputs along with climate scenarios for coupled physical-biogeochemical forecasts in the MS.

Keywords: Mediterranean Sea, River inputs, Coupled physical-biogeochemical model, Flexible stoichiometry model, Biogeochemistry, Nutrient

1. Introduction

The Mediterranean Sea (MS) is a Low-Phosphate Low-Chlorophyll oligotrophic area characterized by a zonal west-east oligotrophic gradient [1]. The two basins, the Western Mediterranean Basin (WMB) and the Eastern Mediterranean Basin (EMB) are characterized by different biogeochemical properties: deep water phosphate (P) and nitrate (N) concentrations as well as primary production are higher in the WMB than in the EMB [2, 3, 4, 5]. Many studies have addressed the issue of nutrient limitation in the MS, and most of them have pointed out the major role of P availability in the control of phytoplankton growth [6, 7, 4, 8, 5] and bacterial production [9, 10], although N [4, 10, 11] and silicate availability [12] could also be limiting factors

in some areas.
At global scale, it is considered that nutrient availability (and especially that of PO_4) in the surface layer of the ocean is mainly controlled by the exchanges between the deep and the upper layers, with a limited influence of river inputs [13, 14]. Nevertheless, as an inland sea, the MS is strongly connected with the Mediterranean continental region. Four main sources of external inputs of nutrients to the upper layer of the MS can be distinguished : the Gibraltar strait connecting the MS to the Atlantic Ocean, the Dardanelle strait connecting the MS to the Black Sea (BS), rivers and runoff and atmosphere (dry and wet deposition). In the WMB, the major external sources of nutrients for the upper layer originate from the Gibraltar strait and from the Rhône and Ebro Rivers. For the EMB, the major sources of nutrients are the Po and Nile Rivers and the Dardanelle strait [15].

Nutrient inputs in the MS have been estimated using *in situ* data and numerical models (see Béthoux et al. [16], Huertas et al. [17] for the Gibraltar strait and Ludwig et al. [15] for rivers and the and Kopasakis et al. [18] for Dardanelle strait (Black Sea)). N and P input from the rivers and the Dardanelle strait have undergone significant changes since the early 1960s [15, 19]: due to human activity, they increased by a factor 5 between the 1960s and the 1980s. After this period of strong increase, N input remained high until 2000, while P rapidly dropped to reach its 1960s value.
Nutrient inputs from Gibraltar have long been considered as the major source of nutrients for the upper layer of the MS compared to river inputs [20, 21, 22], but recent studies have shown that N and P concentrations in the MS are also sensitive to river [23] and atmospheric [24, 25] inputs.

Coupled physical/biogeochemical modeling is particularly suitable for assessing the relative influence of the different nutrient inputs on the biogeochemical cycles of biogenic elements, and on the structure of the planktonic food web in the MS. Several modeling studies at basin or sub-basin scale have already investigated the biogeochemistry of the MS during the last decades [26, 27, 28], but without specific focus on the relative impact of nutrient sources. One exception is [22], who have shown that the atmospheric inputs could be a major source of nutrient in some areas of the MS. However, atmospheric nutrient inputs remain difficult to quantify and their estimation suffers from considerable uncertainty, particularly regarding the bioavailable fraction of these inputs [22, and references herein].

To the best of our knowledge, only two modeling studies have so far highlighted the large-scale influence of river inputs in the MS. [29] show that primary production over the last decades could be impacted by river inputs, but they mostly focus on the link between biogeochemistry and fisheries data. [30] show that in the EMB primary production is sensitive to river inputs, with an increase of 16 % from 1950 to 2000. They also show that the EMB became more P-limited with the reduction of phosphate in anthropogenic nutrient inputs.

In this study, our aim was to address the large-scale and long-term influence of river inputs on the biogeochemistry of the MS over the last decades using an improved version of the coupled physical-biogeochemical 3D model NEMO-MED12/Eco3M-MED [31, 32, 33, 26]. In order to highlight the effect of river inputs alone, two near-identical simulations were run over 25 years (1985-2010 period), the only difference being that one uses the estimated, interannual river inputs provided by Ludwig et al. [15], while in the second, river inputs are fixed to their 1985s level, i.e. before the decline in phosphate discharge.

2. Material and methods

2.1. The biogeochemical model: Eco3M-MED

The biogeochemical model used in this study is embedded in the Eco3M biogeochemical modeling platform, [34] which has been developed with the priority given to (i) mechanistic (i.e. based on underlying processes) descriptions of biogeochemical fluxes [33, 35, 36, 26], and (ii) modularity, with the aim of easy adaptation of the model to different scientific questions (several configurations already exist, some of them dedicated to studies on the Mediterranean Sea [36, 26], others including diazotrophs [37] for studies in the South Pacific, or *Mnemiopsis leidyi* [38] for a theoretical study on the conditions favoring this comb jelly).

The Eco3M-Med configuration has been designed to represent the main characteristics of the Mediterranean Sea. It includes 42 state variables grouped in six different plankton functional types (PFTs), namely two phytoplankton compartments (Large and Small), three zooplankton compartments and a compartment of heterotrophic bacteria. The large phytoplankton (PHYL)(>

$10\mu m$) represents the micro- and the largest nanophytoplankton and is assumed to be mainly composed of diatoms while the small phytoplankton (PHYS) ($< 10\mu m$) includes picophytoplankton and the smallest nanophytoplankton cells. The three PFT of zooplankton correspond to three size classes, namely nano-, micro- and mesozooplankton, which are respectively associated with heterotrophic nanoflagelate (HNF), ciliate (CIL), and copepods (COP). Each PFT, except that for copepods, is described by four state variables, namely Carbon (C), Nitrogen (N) and Phosphorus (P) concentrations, and an abundance (in cell or individuals per liter). Phytoplankton is described by an additional variable (Chlorophyll-a concentration (Chl)), and mesozooplankton is only described through two variables: carbon concentration and abundance. Three pools of inorganic matter are also represented, namely nitrate (NO_3), ammonium (NH_4) and, phosphate (PO_4) as well as a pool of dissolved organic matter (DOM) and two compartments of detrital particulate matter, one including small particles (DETS) and the other large particles (DETL).
The conceptual model (Fig. 1) is the same as that used in Guyennon et al. [26], except that the compartment of detrital particulate matter has been splitted into large and fast-sinking particles (DETL) and small particles (DETS) with low sinking rate. DETL is fueled by the fecal pellets produced by mesozooplankton, and by the mortality of mesozooplankton and large phytoplankton. The hydrolysis of large detrital material, as well as the mortality of CIL, fuel the DETS compartment and the mortality of HNF fuels the DOM compartment. The sinking rates of DETL and DETS are respectively 50 $m.d^{-1}$ and 2 $m.d^{-1}$.

Let X and Y be two biogenic elements among C, N, and P. As in previous versions of the Eco3M-Med model [36, 26], the intracellular ratios ($Q_{X/Y}$) in organisms, as well as their intracellular quotas Q_X (intracellular quantity of X per cell) are flexible and dynamically calculated by the model. These intracellular ratios and quotas are extensively used to regulate the different biogeochemical fluxes represented by the model, and the corresponding equations are given in the previously cited papers.

Only the new features of the model as compared to Guyennon et al. [26] and Gimenez et al. [39] are presented in the appendix.

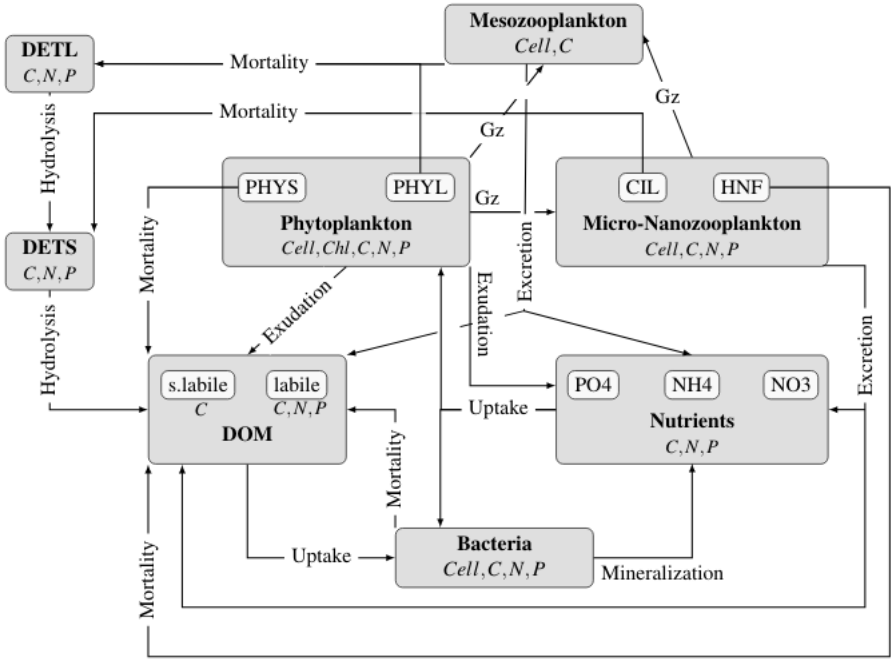

Figure 1: Conceptual model Eco3M-Med.

2.2. The hydrodynamic model : NEMO-MED12

In this study, we use an off-line coupling between the hydrodynamic NEMO (Nucleus for European Modelling of the Ocean) model [31] and Eco3M-MED.
The NEMO-MED12 configuration of NEMO which covers the entire Mediterranean Sea [40] is used. It includes a buffer zone from the Gibraltar strait to 11 degrees east, where the open boundary conditions are gradually applied to avoid numerical instability. The horizontal resolution is 1/12 degree (6.5 to 8 km cells), the vertical resolution has 75 z levels of 1 m width at the surface to 135 m at the seabed.

The hindcast hydrodynamic simulation used in this work is referred to as the NM12-FREE (no reanalysis no data assimilation) which started in October 1979 and ended in June 2013 [32].

In this simulation, the initial conditions for the MS were based on monthly means for temperature and salinity from MEDAR/MEDATLAS [41] and from ORAS4 for the Atlantic part. The runoff and river inputs in the NM12

domain came from the interannual data of [15]. The Black Sea is not included in the NM12 configuration but a fresh water flux from the Dardanelles strait is taken into account [42]. Atmospheric forcing is based on the dynamical downscaling (ALDERA). It has a 12 km spatial resolution and a 3h temporal resolution. For detailed information, the NM12-FREE simulation is extensively described in [32].

2.3. Characteristics of the hindcast simulation

2.3.1. Biogeochemical forcing

River inputs

Monthly values of NO_3 and PO_4 inputs are provided for the 29 main rivers all around the MS by the study of [15]. The contributions of the other rivers were distributed in their respective sub-basins as runoffs. These nutrient inputs are available until year 2000. Between 2001 and 2010, nutrients river inputs of the year 2000 are repeatedly used as already done in [26] and [22]. For dissolved organic carbon (DOC) concentration, an annual mean over every watershed calculated by [43] has been used. In the current configuration, the river discharge is distributed over the six first vertical grid cells. Figure 2 shows the phosphate (PO_4) and nitrate (NO_3) inputs to the MS through river and runoff. It can be seen firstly that nutrient inputs are much higher in the EMB than in the WMB. Moreover, since the end of the 1980s, PO_4 input dropped down from more than 120 to less than 40 kt.a^{-1} in the EMB and from 60 to less than 20 kt.a^{-1} in the WMB. The significant decrease of PO_4 flux reflects the adoption of new legislation by the surrounding countries, such as the prohibition of phosphorus detergents, and the improvement of wastewater treatment plants, as well as other features detailed in Ludwig et al. [15]. By contrast, NO_3 input remains relatively stable over the period.

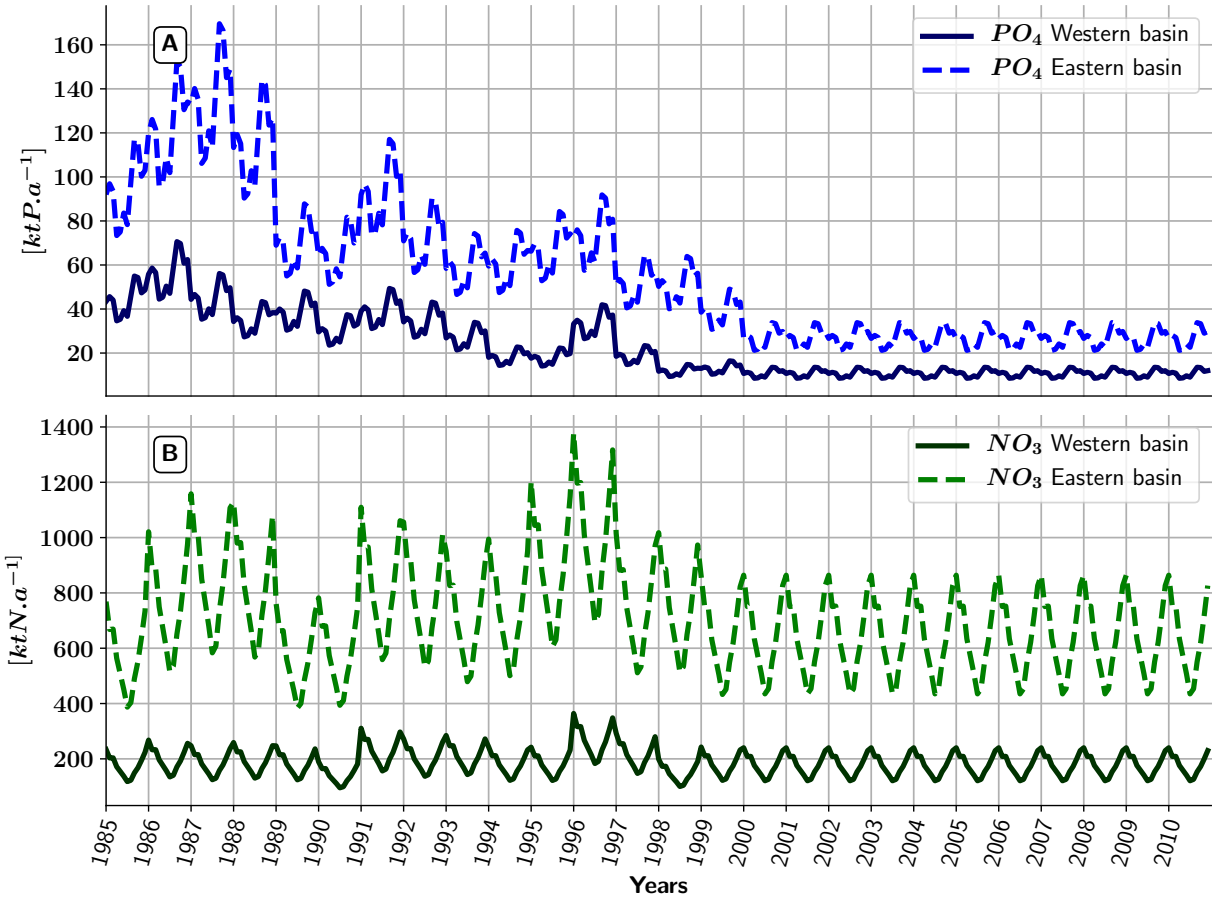

Figure 2: Nutrients inputs from rivers and runoff in $kt.a^{-1}$ [15] used in the model for the eastern basin (dotted line) and for the western basin (plain line). A) PO_4 inputs; B); NO_3 inputs.

Boundary and initial conditions

Nutrient input at Gibraltar is conditioned by the nutrient concentrations in the buffer zone. Annual climatology data (monthly vertical profiles) are used in the buffer zone for each state variable of the biogeochemical model. For PO_4, NO_3, NH_4 and OXY, these annual climatology data are extracted from the World Ocean Atlas database. The other variables have been computed through a mean chlorophyll profile in order to reproduce seasonal variability. They are derived from the profiles using conversion factors derived from

published works [36]. For the initial conditions, the same procedure has been applied. More details on this preliminary work can be found in [44] where it has already been extensively described.

2.3.2. Spin-up and Simulation plans

Using the initial conditions as described before, a first 20-years spin-up was run, consisting in a 5-years simulation (1982-1987) repeatedly run, allowing most of the variables to reach an equilibrium state. Starting from this equilibrium state, the hindcast simulation was run.

In this study, two simulations were run. The first is the hindcast simulation, starting in 1985 and ending in 2010, described in the previous sections. This simulation will be referred to hereafter as the Riv-ref simulation. The second simulation is identical in all respects to the Riv-ref simulation, except that the monthly river inputs of the year 1985 are used throughout the simulation in order to deconvolute the impact of river inputs from other forcing. This simulation is referred to hereafter as the Riv-85.

3. Results

3.1. Model skill assessment

Figure 3 shows the modelled (mCHL) for the Riv-ref simulation and observed (oCHL), i.e. satellite-derived, mean surface chlorophyll *a* concentration over the 1997-2010 period. High chlorophyll clusters can be observed for both oCHL and mCHL in the vicinity of river mouths, but only for oCHL near the Nile, along the western coast of the Adriatic Sea and in the Gulf of Gabes. The well-known east-west gradient of CHL (see oCHL) is also clearly visible in the mCHL pattern. Excluding the coastal areas (i.e. depth < 200 m) which are more impacted by river inputs, the mean chlorophyll concentrations, oCHL and mCHL, are equal to 0.047 and 0.04 $\mu g.l^{-1}$, and to 0.032 and 0.034 $\mu g.l^{-1}$, in the WMB and in the EMB, respectively.

Several similar structures can also be observed in both oCHL and mCHL in the WMB, such as i) a well-defined Liguro-Provencal current, ii) an intense Liguro-Provencal bloom, though slightly more expanded for mCHL than for oCHL, iii) a high-chlorophyll gyre to the south-east of Corsica. For the eastern basin, very low chlorophyll concentrations are observed and modelled, except in the Rhodes gyre where higher concentrations can be seen in both oCHL and mCHL patterns.

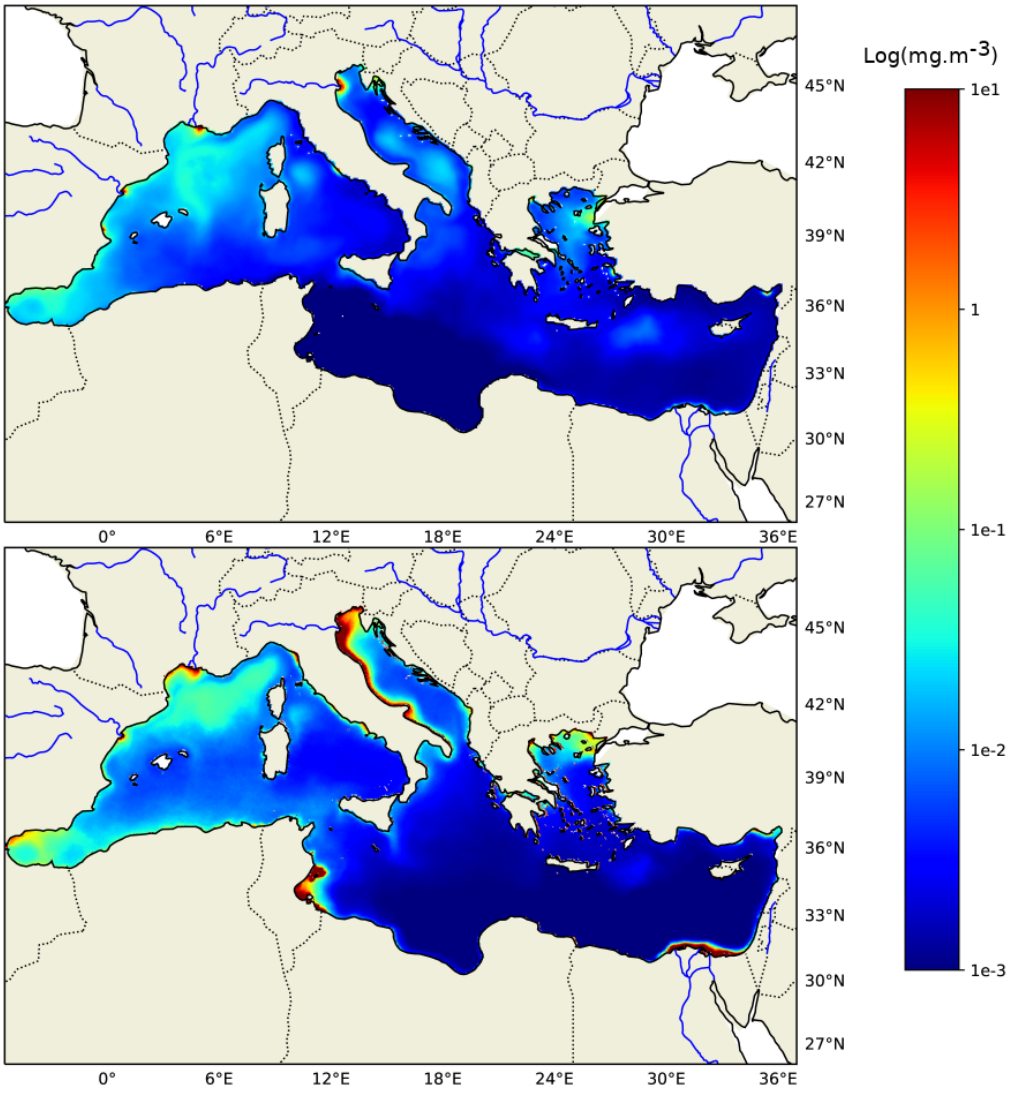

Figure 3: Average surface chlorophyll *a* concentration between 1997 and 2010, (top) calculated by the model and (bottom) observed by satellite.

Overall, the model shows a good ability to reproduce the main structures of surface chlorophyll in the MS, and especially all the main productive areas are detected by the satellite. However, in some areas, Chl structures are not well represented by the model, such as i) the Rhodes gyre where mCHL is too high (+ 0.05 $\mu g.l^{-1}$ than oCHL) , which can be partially ascribed to the too intense convection estimated by the hydrodynamic model in this area [32], ii) the center part of the Adriatic Sea, which is more productive in the model (+ 0.08 $\mu g.l^{-1}$ than oCHL), iii) the coastal Italian side of the Adriatic Sea, which is less productive in the model than in data. This could be due to insufficient PO_4 inputs from the Po river in the model leading to a too strong PO4 limitation of phytoplankton growth, combined with chlorophyll data which are less reliable in case II waters [45], iv) the gulf of Gabes which is less productive in the model (- 0.5 $\mu g.l^{-1}$ than oCHL), where high phosphate supply from the land and the seabed are not taken into account in the model, v) the Nile mouth which is less productive in the model (- 1.06 $\mu g.l^{-1}$ than oCHL) where nutrient input is probably poorly represented because of the lack of data [15].

A quantitative comparison between *in situ* data and model outputs has also been undertaken using a Taylor diagram [47] that shows the standard deviation, the correlation between the data and the model and the root mean square error (Fig. 4). Mean vertical profiles of four biogeochemical variables, dissolved organic carbon (DOC), CHL, NO_3 and PO_4 measured at the Dyfamed station [46] over the 1990-2002 period, are compared with the model outputs averaged over the same period. For CHL, NO_3 and PO_4, correlations are higher than 0.95, with relative standard deviations ranging between 0.78 and 1.2, and an error close to 0.2, showing that the model can predict relatively well those variables at Dyfamed station. For DOC, the comparison with data is less favorable. This could be partly ascribed to the number of available DOC data, which is well below the number of data for the other variables, and to the fact that the comparison is partly biased since Dyfamed data concern the whole DOC pool while the modelled DOC only includes the labile and semi-labile pool. The refractory part of the modelled DOC is therefore arbitrarily set to a constant value for the comparison with *in situ* data, thereby introducing a systematic error. These comparisons and others not shown led us to conclude that the model was able to reproduce

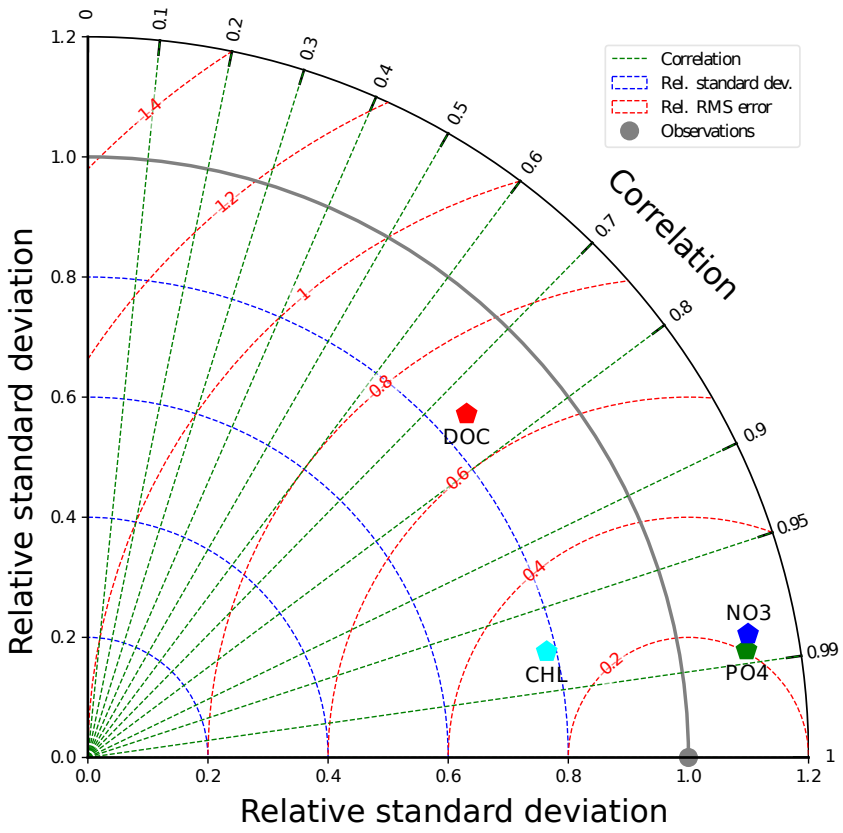

Figure 4: Taylor diagram showing the standard deviation of the normalized model outputs, the correlation between *in situ* data and model outputs, and the root mean square error between in situ data and model outputs. Data consist in vertical profiles of NO_3, PO_4, DOC and CHL obtained at Dyfamed [46] station during the period 1990-2002. Model outputs are vertical profiles averaged over the same period. In red: dissolved organic carbon (DOC), in light: blue chlorophyll *a*; in green: PO_4 and in blue: NO_3.

most of the major biogeochemical features of the MS and could be used to investigate the effects of the variations in nutrient concentration in the river inputs.

3.2. River input and the biogeochemistry of the MS

3.2.1. Nutriclines

According to the model, over time, the evolution of continental nutrient inputs has various effects on the biogeochemistry of the MS.
One of them concerns nutriclines, and more specifically the top of nutriclines. Let us first define how the top of the nitracline (Ncline) and phosphacline (Pcline) are determined. The top of the Ncline is located at the first depth, starting from the sea surface, at which NO_3 reaches 0.05 μmol.l^{-1}. This threshold corresponds to the classical quantification limit of nitrate measurement using an autoanalyser [48].Such determination of the top Ncline has already been used by Pujo-Pay et al. [2] and Bahamón et al. [49].

The depth of the top of the Pcline is based on a threshold value of 3 nmol.l^{-1}. The latter value corresponds to the nitrate threshold (i.e. 0.05 μM) divided by 16, that is, by the Redfield proportion between N and P. Figure 5 shows the patterns of change over time of the top of the Pcline for the WMB (A) and the EMB (B) over the period 1985-2010. There is no clear trend over this period in the WMB (Fig. 5 A). The top of the Pclines seasonally reaches the surface in winter and deepens to around 60 m in Summer (Fig. 5 A). In the EMB (Fig. 5 B), the top of the Pcline never reaches the surface, not even during winter convection. Moreover, there is a clear trend towards a deepening of the Pcline between the 1980s and the year 2000s. This deepening can be better quantified in figure 5 D where the difference between the depths of Pcline for the Riv-ref simulation (using realistic changes in river input) and the Riv-85 simulation is reported for the EMB. It can be seen there that the the top of the Pcline can deepen as far as 40m. A similar result (not shown) is obtained for the 0-150 m integrated PO_4 concentration (referred to as I - PO_4 hereafter). In the WMB, this deepening is far less marked, that is less than 10 m (Fig. 5 C). Concerning the top of the nitracline (not shown), it exhibits the same seasonal variations as the Pcline, but no clear trend could be evidenced, either in the WMB, or in the EMB.

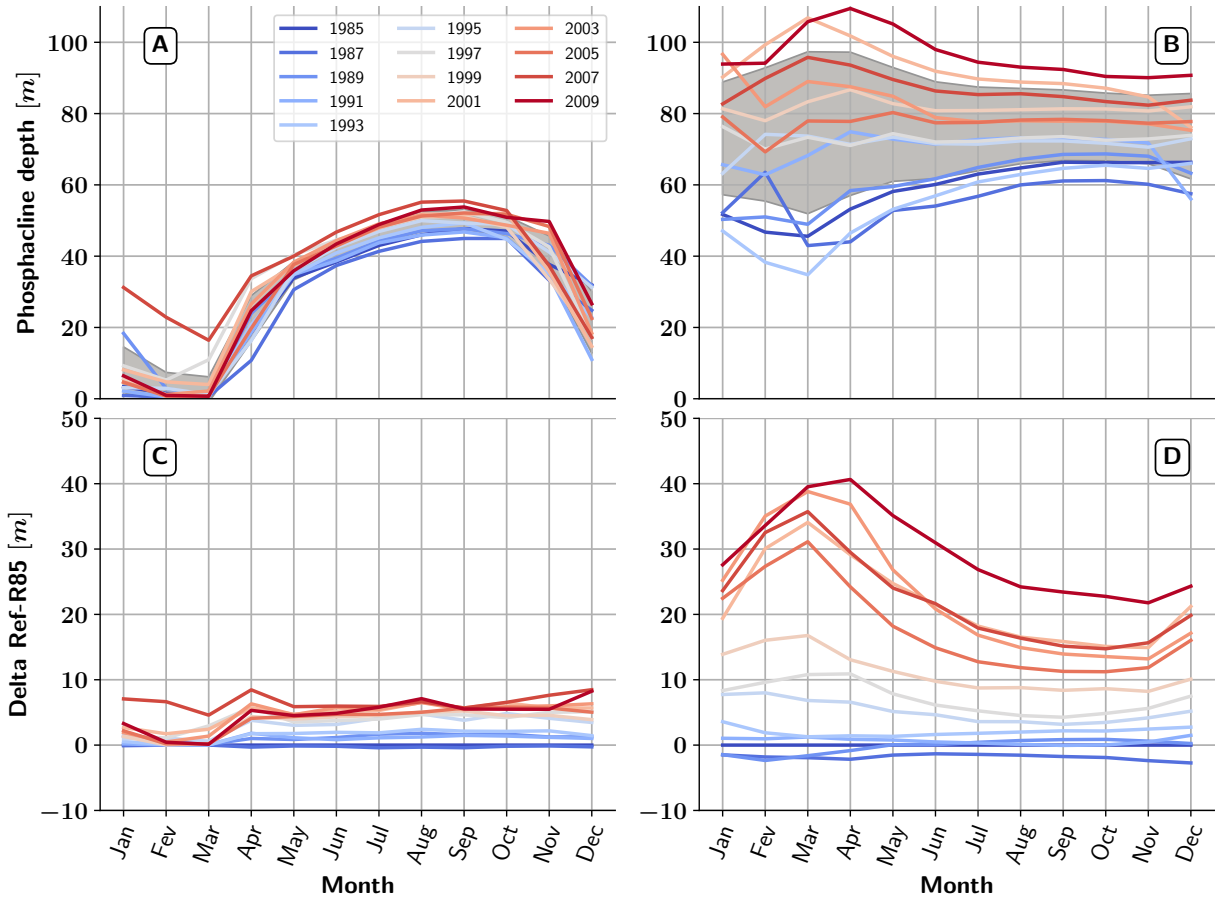

Figure 5: Patterns of change in the depth of the top of the phosphacline (see the definition in the text) for (A) the western basin and (B) the eastern basin and difference between the top of the phosphacline for the Riv-ref and the Riv-85 simulations for the (C) western basin and (D) the eastern basin over the period 1985-2010. Each line corresponds to a two-year average. The line colors progressively change from blue (1985) to red (2010) in order to highlight the temporal changes during that period. The grey area delimits the maximum standard deviation of the 1985-2010 averaged depth of Pcline (throughout period 1985-2010).

In the model, the biogeochemical processes controlling the depth of the Pcline are the different production and consumption fluxes: uptake of PHYS (Fig. 6 A); uptake of PHYL (Fig. 6 B); uptake of BAC (Fig. 6 C); excretion of CIL and HNF (Fig. 6 D) and mineralization by BAC (Fig. 6 C). The mean depth at which production and consumption fluxes of PO_4 are balanced is

also represented (Fig. 6 F). PO_4 uptake by PHYS in the upper surface (0-50 m) decreases from $0.6 \pm 0.1 \times 10^{-15}$ mol.l^{-1}.s^{-1} in 1985 to $0.89 \pm 0.1 \times 10^{-16}$ in 2010 (Fig. 6 A). The maximum uptake rate, corresponding to the maximum abundance (not shown), is a little bit weaker and deeper in 2010. For PHYL, the maximum uptake decreases from $3.3 \pm 0.1 \times 10^{-16}$ in the 1980s to $5.14 \pm 0.1 \times 10^{-17}$ mol.l^{-1}.s^{-1} in the years 2000s (Fig. 6 B). PO_4 uptake by bacteria (Fig. 6 C) decreases only at the surface and becomes deeper over the years. The maximum uptake deepens slightly between 1985 and 2010, but its intensity remains stable around 4×10^{-14} mol.l^{-1}.s^{-1}.

The excretion by microzooplankton (CIL) and nanozooplankton (HNF) decreases progressively over the period (Fig. 6 D) and the maximum excretion deepens (though this is barely visible in this figure). The maximum remineralization by heterotrophic bacteria also deepens from less than 200 m in the 1980s to almost 300 m in the years 2000's and is also less intense (Fig. 6 E). The depth where a balance between production and consumption fluxes is reached also deepens from 200 m in 1985 to almost 300 m in 2010 (Fig. 6 F).

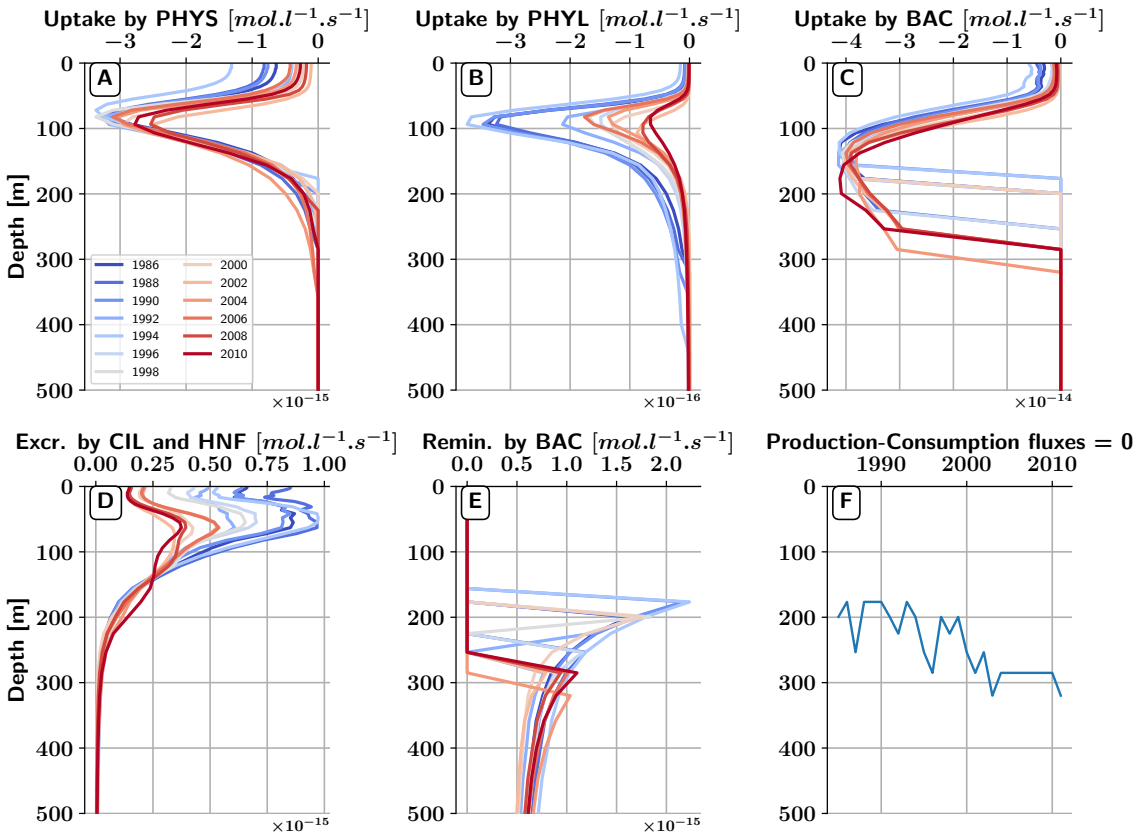

Figure 6: Patterns of change in the different production and consumption fluxes of PO_4 playing a role in the position of the phosphacline in the eastern basin; A) Uptake by small phytoplankton; B) Uptake by large phytoplankton; C) Uptake by bacteria; D) Excretion by micro and nanozooplankton; E) Remineralization by bacteria; F) Depth where a balance between production and consumption fluxes is reached.The line colors progressively change from blue (1985) to red (2010) in order to highlight the temporal changes during that period. Negative values refer to fluxes from water towards organisms and positive ones from organisms towards water.

3.2.2. Surface Dissolved Organic Carbon

Surface DOC concentration exhibits a clear seasonal pattern, not only for the WMB (Fig. 7 A) but also for the EMB (Fig. 7 B). To highlight a potential trend in surface DOC concentrations over the 1985-2010 period, the difference between DOC concentration for the Riv-ref and the Riv-85 simulations is plotted for the two basins. The trend is tenuous in the WMB (Fig. 7 C), while there is a regular and significant DOC concentration increase of nearly

311 20% in the EMB over the same period (Fig. 7 D).

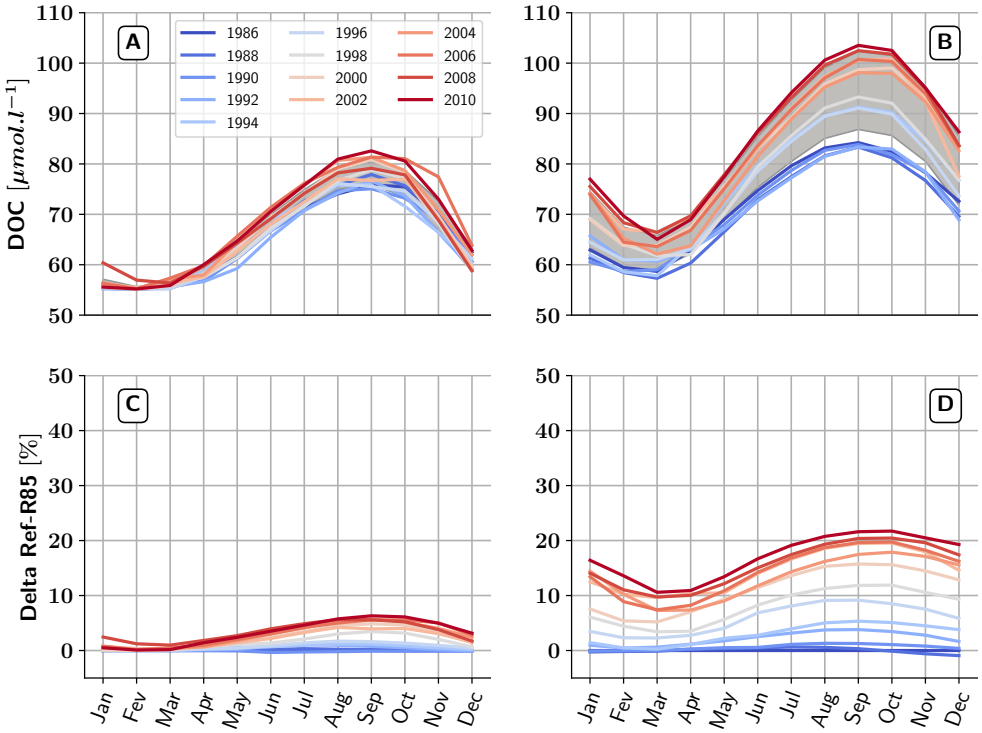

Figure 7: Patterns of change in surface DOC concentration in μmol.l^{-1} for (A) the western basin and (B) the eastern basin and difference between the top of the phosphacline for the Riv-ref and the Riv-85 simulations for the (C) western basin and (D) the eastern basin over the 1985-2010 period, as calculated by the model. The line colors progressively change from blue (1985) to red (2010) in order to highlight the temporal changes during that period.

312

3.2.3. Time and spatial distribution of certain biogeochemical variables at basin scale

Figure 8 shows that during the simulated period, I-PO_4 drops everywhere in the EMB (Fig. 8), except near the Sicilian strait and to the south of Rhodes due to very strong and deep vertical mixing. This decrease in I-PO_4 can be as high as 40 % (Fig. 8). In the WMB, the spatial variability of the difference in I-PO_4 between 1985 and 2010 is slightly more noticeable but remains weak. The difference in I-PO_4 remains close to 0 % except near the coastal areas where the decrease in I-PO_4 over the period can reach up to 30 %, and offshore of the Gulf of Lions where I-PO_4 is higher in 2010 than 1985. It can also be seen that DOC concentration at the surface progressively increases between 1985 and 2010 in the EMB (Fig. 8) and reaches more than 40 % in some areas, while DOC concentration remains nearly constant in the WMB.

The patterns of change over with time of the 0-150 m integrated carbon biomass of copepod (I-COP-C) is also reported in the same figure, showing that I-COP-C decreases mostly in the EMB between 1985 and 2010 (Fig. 8). In the same period, we observe a decrease in COP abundance (not shown). Furthermore, I-COP-C exhibits wide mesoscale variability over the MS (Fig 8) with a decrease in the EMB in coastal areas and an increase in the gulf of Gabes and near the Algerian coast. This result highlights the importance of mesoscale activity with regard to the biogeochemistry of the Mediterranean sea.

4. Discussion

4.1. The decrease in PO_4 input by rivers strongly impacts the biogeochemistry of the eastern basin

The hindcast simulation over the period (1985-2010) using the coupled model NEMO-MED12/Eco3M-Med shows a significant decrease in the 0-150 m integrated PO_4 concentration (I-PO_4), especially in the EMB (Fig. 8). At first glance, several factors could explain this decrease, namely (i) a drift of the model, (ii) changes in PO_4 surface inputs at Gibraltar strait, (iii) changes in the vertical exchanges between the upper and the deep layers, or (iv) changes in river input and runoff, or possibly a combination of all these factors. The three former causes have been ruled out: it has been verified

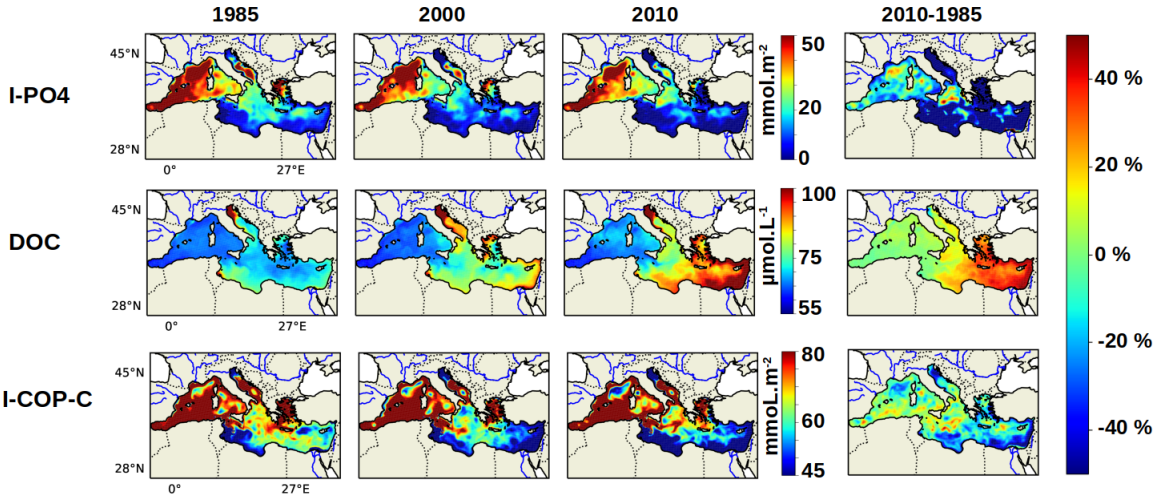

Figure 8: Patterns of change at basin scale between 1985 and 2010 of: (top) the 0-150 m integrated PO_4 concentration(I-PO_4), (middle) the surface DOC concentration, (bottom) the carbon biomass of copepods (I-COP-C) integrated between 0 and 150 m. The first three columns refer to the years 1985, 2000 and 2010, respectively, and the last column shows the difference between 1985 and 2010 (i.e 2010 value - 1985 value)

first that the model drift was negligible after having run the spin-up, and that PO_4 surface inputs at Gibraltar strait were approximately constant during the simulated period. Concerning vertical mixing, it has been confirmed that the mean position of the mixed layer depth (MLD) did not significantly vary over this period, that the seasonal and annual standard deviation of the ML did not show any trend, and that vertical velocities as well as the vertical eddy diffusivity at the bottom of the ML did not exhibit any trend either. As a result, changes in river input and runoff is the only factor in the model able to explain the decrease in integrated PO_4 concentration in the EMB. In order to confirm this assumption, a twin simulation only differing by nutrient input from rivers and runoffs has been run. In the second simulation, PO_4 input remains at the 1985s level.

The comparison between the two simulations confirms the major influence of changes in PO_4 river input and runoff on the integrated PO_4 concentrations and beyond on the MS biogeochemistry, especially in the EMB. The decrease in I-PO_4 probably results from the combination of a direct and an indirect effect. The direct effect is a consequence of the decrease in PO_4 input

by Mediterranean rivers between 1985 and 2000 [15]. PO_4 input from rivers and runoff strongly decreased during this period in the WMB and in the EMB (see Fig. 2), while NO_3 input remained roughly unchanged. Moreover, this decrease is stronger in the EMB: PO_4 inputs indeed decreased from 140 $kt.a^{-1}$ to less than 40 $kt.a^{-1}$ between the 1980s and the 2000s in the EMB, and from 50 $kt.a^{-1}$ to less than 20 $kt.a^{-1}$ in the WMB during the same period.

Overall, the model shows, on time scales of a few decades, a strong relationship between nutrient input via rivers and nutrient availability in the surface layer, as already pointed out by Powley et al. [30], as well as the link between the decrease in PO_4 input by rivers and the increase of P depletion in the EMB. It is nevertheless in contradiction with the study of [14] showing similar annual PO_4 input by the Rhône River and annual PO_4 storage in the upper sediment of the Gulf of Lions, indicating no strong influence only close to the river mouth of one of the major rivers in the MS.

Furthermore, a decrease in surface PO_4 has been recently reported in the Levantine basin [50]. This decrease is however rather a shift in phosphate concentrations than a progressive decrease over years, which may be caused by decadal reversals in the North Ionian Gyre, i.e. Bimodal Oscillation System (BiOS). Such alterations of the MS circulation, as well as many other factors that are not necessarily included or well represented in our model may indeed contribute to an impact on the biogeochemistry of the MS. However, considering that our results rely on two identical simulations only differing by river inputs and runoff, the unavoidable inaccuracies in the aforementioned model do not call into question the unexpected conclusions they lead to on the major influence of river inputs on the biogeochemistry of the MS.

The indirect effect of changes in PO_4 river input and runoff is the deepening of the top of the phosphacline (i.e. Pcline as defined in section 3.3) which occurs only in the EMB (from 60 m in 1985 to 90 m in 2010). This deepening exacerbates the decrease in PO_4 in the surface layer by restricting the PO_4 flux brought to the surface through winter mixing. Investigating the reasons for this deepening requires to describing in detail all PO_4 fluxes shaping the Pcline. The position of the Pcline within the water column (during stratified conditions) results from an equilibrium between PO_4 production and consumption fluxes [3, 2, 51].

The consumption of PO_4 in the model is driven by PHYS, PHYL and

BAC uptake. Phytoplankton and bacteria need nutrients (NO_3, PO_4) to grow, as well as carbon. Carbon essentially comes from DIC uptake (photosynthesis) by phytoplankton and from DOC uptake by heterotrophic bacteria [52]. This uptake progressively decreased over time in surface waters because of the gradual depletion of PO_4 (Fig. 6). The maximum PO_4 uptake rates at depth (around 100 m) for PHYS and PHYL also decrease with time, mostly for PHYL (Fig. 6) because sufficient nutrient concentrations to sustain the growth of organisms are only found at greater depth. However, the efficiency of photosynthesis decreases with depth since light energy decreases as well, leading to an increase in carbon limitation for phytoplankton and to lower cell abundance, and in turn to a decrease in nutrient uptake rates.

PHYL is more sensitive to nutrient variations in the model. Because of the scaling relationship between nutrient uptake and organism size [53], PHYL is characterized by a higher half-saturation constant than PHYS [33], making it less adapted to ultra-oligotrophic conditions. The uptake of BAC is deepening over the period (Fig. 6 c) but it does not strongly decrease at depth since, unlike phytoplankton, bacteria use DOC as carbon source and are therefore not limited by light. Bacteria follow the deepening of the Pcline as long as labile DOC is available.

PO_4 is produced by zooplankton excretion and bacteria remineralization. Excretion of CIL and HNF is regulated by Q_P, their intracellular P quota (i.e. excretion non-linearly increases with Q_P). Since the abundance and the Q_P of CIL and HNF's preys (namely PHYS and BAC for HNF, and PHYS, BAC and HNF for CIL) decline over the period (not shown), the Q_P of CIL and HNF decrease as well. As a result, PO_4 excretion by HNF and CIL decreases. The deepening of PO_4 production by BAC remineralization could also be explained by the P quota of BAC. BAC reach their maximum P quota (i.e. the value allowing remineralization of organic P) deeper because of the increasing P depletion in the surface layer. Moreover, the decrease in remineralization intensity with depth is also due to the diminution of BAC abundance associated with the lower concentration of labile DOC at depth.

To sum up, PO_4 consumption fluxes show a clear decreasing trend in the surface layer while the maximum of consumption deepens and its intensity remains almost unchanged. PO_4 production fluxes also show a clear decreasing trend in the surface layer, as well as in depth. As a result, the equilibrium between all those processes occurs deeper in the water column, resulting in a Pcline that deepens over the years. Furthermore, the amount of PO_4 brought

to the surface layer annually during winter mixing also decreases, thereby reinforcing the lower availability of PO_4 in the surface layer.

To the best of our knowledge, no deepening of the top of the phosphacline in the EMB during the last decades has yet been reported in the literature. The lack of data and the quantification limit issue associated with PO_4 measurement probably explains why this question has not been addressed so far. We gathered the few available NO_3 and PO_4 data recorded in the center of the Levantine Sea and collected during five cruises over our simulation period, namely POEM 05 (1987), LBD01 (1989), MINOS (1996), PROSOPE (1999) and BOUM (2008). The vertical PO_4 and NO_3 profiles measured during these cruises have been reported in figure 9 in order to test the hypothesis of the deepening of the Pcline using *in situ* data. According to the POEM and BOUM cruises data, PO_4 concentration between 100 and 200 m seems to decrease between 1987 and 2008 while NO_3 concentration remains constant during the same period. Given the limited set of data available in the open EMB, and taking into account the issue of the relatively high quantification limit for PO_4 measurements, those data are obviously not a sufficient basis for any definite conclusions, but they do however seem to confirm the deepening with time of the top phosphacline simulated by the model, as well as the roughly constant position of the top nitracline.

In the model, the fact that only the top Pcline deepened in the EMB between 1985 and 2010 results in the appearance of a shift between Pcline and Ncline which increases with time. During the BOUM cruise in 2008, [2] measured a maximum shift between nutriclines of 130 m in the Levantine basin, and a mean shift of around 60 m if we exclude the eastern stations sampled in the center of an anticylonic eddy characterized by specific hydrodynamic conditions [1]. To calculate the position of the top of the nitracline [2] use, as we do (see section 3.3), the threshold of 0.05 μmol.l^{-1}, leading to a mean nitracline top located at approximately 75 m, which is consistent with the top of the nitracline depth calculated by our model (between 70 m and 75 m). For the determination of the depth of top of the phosphacline, [2] use the threshold value of 0.02 μmol.l^{-1}, resulting in a mean top phosphacline depth at around 130 m if we exclude the eastern stations for the reason previously mentioned. In the model, we find a phosphacline top depth at around 90 m in the EMB with the more restrictive threshold of 0.003 μmol.l^{-1}. However,

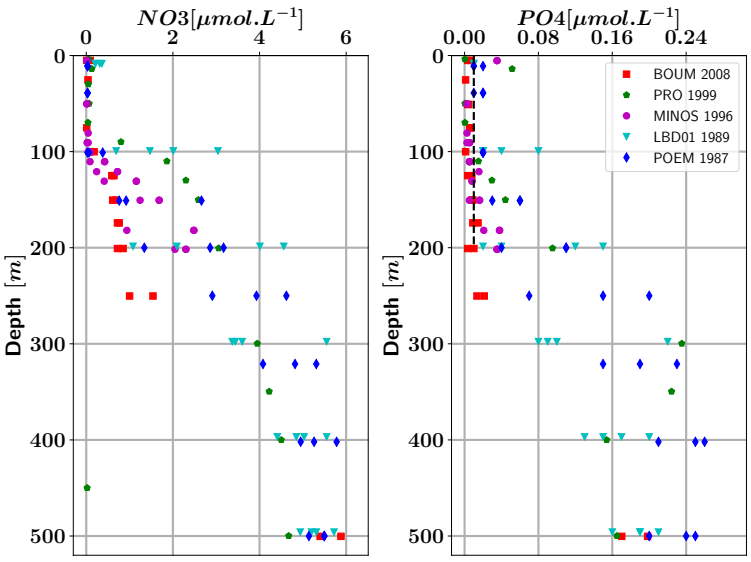

Figure 9: NO_3 (left) and PO_4 (right) data from five cruises in an area located in the center of the Levantine sub-basin, namely : i) POEM 05 (June 1987) in blue; ii) LBD01 (April 1989) in cyan; iii) MINOS (June 1996) in pink; iv) PROSOPE (September 1999) in green; v) BOUM (July 2008) in red. The black dotted line shows the quantification limit, except for the BOUM cruise during which sensitive methods of analysis were used.

if we apply the same threshold value as [2], the model calculates a phosphacline top depth between 110 and 125 m in the EMB, which is consistent with *in situ* data.

The shift between the top of nutricline depths in the EMB has been previously reported in literature [4, 54, 2] and explained by several processes but changes in river input were never suspected of playing a significant role in this shift. So far, the most common explanation for this shift (and for the associated high subsurface NO_3:PO_4 ratio) was related to the high deep NO_3:PO_4 ratio, i.e. higher than the Redfield value, as a result of nutrient budgets regulated by nutrient exchanges at straits, and especially at the Gibraltar strait [55]. Upward diffusion of deep nutrients taken up biologically at a constant molar N:P ratio of 16:1 may theoretically lead to subsurface ratios as high as those observed at depth [7, 4]. External atmospheric inputs were also recently suggested to play a role in the high surface and subsurface NO_3:PO_4 ratio [25, 24].

This study suggests that the N:P ratio in nutrient input by rivers, and its

deviation from the Redfield ratio, may partly explain the shift between the top of the nitracline and phosphacline in the MS as a result of a deepening of the Pcline (due to the strong decrease in PO_4 inputs from rivers), without a similar deepening in the Ncline.

4.2. Patterns of change in DOC concentration between 1985 and 2010 and consequences for the biological carbon pump

DOC surface concentration increases strongly over the simulated period, especially in the EMB (Fig. 7 and 8). At the scale of the EMB, this increase reaches 20 % (Fig. 8) but it is far higher in the Levantine sub-basin, reaching there more than 40 %. An inverse trend for PO_4 concentrations was observed (Fig. 8) reinforcing the west to east oligotrophy gradient in the EMB.

This increase in DOC is driven by the same mechanisms as those involved in the surface DOC accumulation observed every summer in the MS [8, 9]. The latter, namely an increase in DOC exudation by P-limited phytoplankton exceeding bacterial DOC demand, since bacteria are also strongly P-limited, have already been extensively described in Guyennon et al. [26]. Over the simulated period, the EMB upper waters become more and more P-depleted (Fig. 8) which induces a rise in DOC exudation by phytoplankton (Fig. 8). Furthermore, because of the strong P-limitation of both phytoplankton and heterotrophic bacteria, the abundance of bacteria decreases in the surface layer, as has been evidenced *in situ* [9]. The decrease in bacterial abundance probably also leads to a decrease in DOC consumption by bacteria and reinforces DOC accumulation.

A DOC concentration increase between 1985 and 2010 cannot be validated with any certainty since very few DOC measurements in the EMB before the years 2000 are available, and most of them were carried out in coastal areas. Moreover, as already mentioned, the comparison is not easy since DOC *in situ* data refer to total DOC, while the modelled DOC does not include the refractory part, making necessary an approximation for refractory DOC. Overall, the model seems to provide realistic DOC values as suggested by comparison with *in situ* data from the DyFaMed station over the 1992-2002 period (see Fig. 4) or from the BOUM cruise (not shown). The modelled increase in dissolved organic carbon is not observed in the detrital particulate carbon, which even slightly decreases. However the total organic carbon increases, indicating that the pool of organic carbon available for export has increased during the period. Since, as already shown by [26], the export of DOC in the eastern basin is the main component of the exported organic

carbon, the strong DOC increase in the EMB has significantly increased DOC export during this period.

4.3. A simulated decrease in mesozooplankton abundance and biomass with expected consequences for higher trophic levels

Despite the wide variability associated with mesoscale activity (Fig. 8), a strong decrease in biomass (I-COP-C) and abundance of copepods was modelled in the EMB, as well as in the offshore part of the WMB, between 1985 and 2010. The carbon intracellular quota (Q_C) of COP decreases as well in the same regions. In the model, COP are the top predators. Their intracellular carbon is directly related to the abundance and the carbon content of their prey, namely PHYL, CIL and HNF, with a preference for PHYL over the two others. Because of strong phosphate limitation, abundance of PHYL decreases (not shown), thereby limiting the number of prey available for COP. The abundance of HNF and CIL also decreases, because of the decrease in prey abundance. Such depletion of COP preys explains the decrease in COP biomass and abundance. A similar decreasing trend in COP abundance due to increasing land-based N:P nutrient load has already been observed in the San Francisco Estuary Bay Delta [56].

The decrease in COP abundance could have a significant effect on small pelagic fishes such as sardine and anchovy. Copepods are indeed an important link in marine food webs as prey for larger pelagic predators [57]. As an example for the MS, [58] highlighted changes in biomass and fish mean weight of sardine and anchovy in the Gulf of Lions around 2008. They showed that the bottom-up control exerted by the plankton community played an important role in those changes through a decrease in fish energy income. They also showed that copepod abundance was directly linked to fish characteristics (size and weight). Those results are difficult to reproduce with our model since the Gulf of Lions is too small and too coastal an area with regard to the size of the horizontal grid used, but they nevertheless seem to confirm the general trend predicted by the model at larger scale. In the same way, [59] showed a decrease in the mean length of sardines between 1996 and 2000 in the EMB. They pointed out that, among other factors, the quality of their preys (among which copepods) could have decreased, leading to a diminution of the size of sardine. This could be linked to the decrease in COP abundance and Q_C predicted by the model (Q_C can indeed be seen as a proxy of the nutritional quality of copepods and of their size) during the same period and at least partially explained by the changes in river outputs

during the last decades. Furthermore, this suggests that COP abundance and Q_C, as calculated by the model, could be used as one indicator among others of the stocks and size of small pelagic fish in the MS in future modeling scenarios.

5. Conclusion

This study provides new insight into the possible effects of changes in nutrients provided by river inputs on the biogeochemistry of the MS over the last decades. The strong reduction of PO_4 input by river and runoffs, that occurred over the last decades in the EMB, induces a lowering of PO_4 availability in the sub-surface layer of this basin. An indirect consequence of these strong variations in river inputs lies in the deepening of the top of the phosphacline, as an adjustment of organisms and biogeochemical cycles to the sub-surface PO_4 decrease. Since the position of the top of the nitracline remains unchanged during that period, a shift between the two nutriclines gradually emerges. This provides a new explanation for the shift between the top of the nutriclines already mentioned in literature.

Another result provided by this modelling study concerns the rise of the DOC concentration in the surface layer between 1985 and 2010, as evidenced by the model in the EMB. The increasing P limitation in this basin results in higher DOC accumulation in the surface layer, and therefore in increasing DOC export fluxes over the last decades (not shown). This is of major importance since DOC export represents the major part of the total (dissolved and particulate) carbon export in the MS, as has been evidenced in Guyennon et al. [26].

Finally, we have highlighted the decline over the years 1985-2010 in copepod abundance and intracellular content, the latter being a proxy of copepod size. Those decreases could have had an important impact on the higher trophic levels, and potentially provide an explanation to the smaller size of sardine or anchovy recently observed in the MS. Broadly speaking, the model underlines a trend towards the decline of large organisms in favour of small organisms.

Overall, this study emphasizes the fact that the biogeochemistry of the two basins of the MS did not exhibit the same response to the variation of rivers inputs. Significant biogeochemical trends were simulated over the period 1985-2010 in the eastern basin. By contrast, the WMB seems to be less sensitive to changes in river inputs, but it is difficult within the scope of this study, to determine whether this is due to the difference in the characteristics of the two basins, or whether it is due to the lower variations observed in river inputs in the WMB as compared to those in the EMB. It is probably a combination of these two factors. It has also been evidenced that these variations in river inputs and runoff may affect not only the coastal areas

and the direct vicinity of river mouths, but also offshore areas. Finally, the magnitude of the biogeochemical changes induced by river inputs and runoff alone over the last thirty years clearly calls for the use of realistic scenarios of river inputs along with climate scenarios for coupled physical-biogeochemical forecasts in the MS.

Acknowledgements

This study has been made possible thanks to a PhD thesis funded by the LaSeR-Med project. This project is part of the Labex OT-Med (no. ANR-11-LABX-0061) funded by the French Government "Investissements d'Avenir" program of the French National Research Agency (ANR) through the A*MIDEX project (no ANR-11-IDEX-0001-02). This study has been conducted using E.U. Copernicus Marine Service Information. This work was performed using HPC resources from GENCI-IDRIS (Grant 2018-0227).

Appendix A. New features of the biogeochemical model

Since the Alekseenko et al. [36] first version of the Eco3M-Med model, some features of the original model were improved and some new features were introduced to correct the model major flaws or to add some realism to the model. In [26], it has been shown that the position of the nitracline and the phosphacline were not well represented by the model (Figures S3 and S4 in the Supplement). A deep work has then been undertaken on the remineralization process which was up to now function of the N:C and P:C ratios in bacteria. In the present version of the model, the outflow of N and P associated with the uptake of dissolved organic matter (DOM) is still function of the N:C and P:C intracellular ratios (i.e. it is maximum when the N:C or the P:C ratio takes its maximum value), but the intracellular carbon quota Q_C will redirect this outflow either towards the DOM pool when Q_C is high or towards the mineral pool otherwise. Concerning parameters, in [39], the half-saturation constants (Ks) for the DOP uptake were divided by 1 order of magnitude in order to better match in situ data. However, Ks values in the original model were all calculated using a similar method and mechanistic considerations based on the shape of cells and the control of the uptake rate by molecular diffusion at low nutrient concentrations. Here, we consider a more realistic cells shape to derive new values of the Ks for NO_3, NH_4, PO_4, LDON and LDOP involved in the model in a similar way. Using the diffusion flux established by Kiorboe [60] for cigare-shaped (ellipsoid) cells, we derive the following relationship between the maximum uptake rate (V^{max}) of a given nutrient and the associated half-saturation constant as done in Mauriac et al. [35]:

$$K_s = \frac{V^{max} Ln(\frac{2a}{b})}{4\pi \mathcal{D} a} \tag{A.1}$$

where a and b stand for the semiaxes of the cigare-shaped ellipsoid ($a^2 >> b^2$) and $\mathcal{D}$ for the molecular diffusion coefficient (see Tab. Appendix A).

Table A.1: Parameters for the half-saturation constant

Variable	Value
$\mathcal{D}_{NO_3}$ diffusion coefficients $[m^2.s^{-1}]$	$1.7\ 10^{-9}$
$\mathcal{D}_{PO_4}$ diffusion coefficients $[m^2.s^{-1}]$	$7.5\ 10^{-10}$
$\mathcal{D}_{NH_4}$ diffusion coefficients $[m^2.s^{-1}]$	$1.9\ 10^{-9}$
$\mathcal{D}_{DON}$ diffusion coefficients $[m^2.s^{-1}]$	$3.0\ 10^{-10}$
$\mathcal{D}_{DOP}$ diffusion coefficients $[m^2.s^{-1}]$	$3.0\ 10^{-10}$

649 Table Appendix A gives the values for a associated which each functional
650 group. The ratio a/b has been set to 10. Finally, the K_s values derived from
651 Eq. A.1 provide a consistent set of K_s values and they were all multiplied
by the same number (50) to match the range given by literature.

Table A.2: Parameters for the half-saturation constant

Variable	PHYL	PHYS	BAC
a Semi major axis of the ellipsoid $[\mu m]$	$2\ 10^{-5}$	$2.5\ 10^{-6}$	$4\ 10^{-7}$

652

Other parameter values were modified (see table A.3), either to improve the consistency between the model parameters (for photosynthetic parameters), or to better integrate the knowledge from literature (hydrolysis rates), or to improve the model outputs (costs of DOC uptake, sinking rates).

Table A.3: Other parameters

Variable name	Value
PHYL PSII cross section [$m^2.J^{-1}$]	2.5
PHYS PSII cross section [$m^2.J^{-1}$]	2.0
MOPL specific hydrolysis rate [d^{-1}]	15
MOPS specific hydrolysis rate [d^{-1}]	7.5
Sinking rate of MOPL [$m.d^{-1}$]	50
Sinking rate of MOPS [$m.d^{-1}$]	2.0
Cost of DOC uptake	0.15
Cost of SLDOC uptake	0.25

References

[1] T. Moutin, F. Van Wambeke, L. Prieur, Introduction to the Biogeochemistry from the Oligotrophic to the Ultraoligotrophic Mediterranean (BOUM) experiment, Biogeosciences 9 (2012) 3817–3825.

[2] M. Pujo-Pay, P. Conan, L. Oriol, V. Cornet-Barthaux, C. Falco, J. F. Ghiglione, C. Goyet, T. Moutin, L. Prieur, Integrated survey of elemental stoichiometry (C, N, P) from the western to eastern Mediterranean Sea, Biogeosciences 8 (2011) 883–899.

[3] G. Crispi, R. Mosetti, C. Solidoro, A. Crise, Nutrients cycling in Mediterranean basins: the role of the biological pump in the trophic regime, Ecological Modelling 138 (2001) 101–114.

[4] T. Moutin, P. Raimbault, Primary production, carbon export and nutrients availability in western and eastern Mediterranean Sea in early summer 1996 (MINOS cruise), Journal of Marine Systems 34 (2002) 273–288.

[5] I. Siokou-Frangou, U. Christaki, M. G. Mazzocchi, M. Montresor, M. Ribera D'Alcala, D. Vaque, A. Zingone, Plankton in the open mediterranean Sea: A review, Biogeosciences 7 (2010) 1543–1586.

[6] M. D. Krom, S. Brenner, L. I. Gordon, Phosphorus limitation of primary productivity in the eastern Mediterranean Sea, Limnology and Oceanography 36 (1991).

[7] F. Diaz, P. Raimbault, B. Boudjellal, N. Garcia, T. Moutin, Early spring phosphorus limitation of primary productivity in a NW Mediterranean coastal zone (Gulf of Lions), Marine Ecology Progress Series 211 (2001) 51–62.

[8] T. F. Thingstad, M. D. Krom, R. F. Mantoura, G. A. F. Flaten, S. Groom, B. Herut, N. Kress, C. S. Law, A. Pasternak, P. Pitta, S. Psarra, F. Rassoulzadegan, T. Tanaka, A. Tselepides, P. Wassmann, E. M. S. Woodward, C. W. Riser, G. Zodiatis, T. Zohary, Nature of P limitation in the ultraoligotrophic Eastern Mediterranean. Supporting Material, Water (2002) 1–10.

[9] F. Van Wambeke, U. Christaki, A. Giannakourou, T. Moutin, K. Souvemerzoglou, Longitudinal and vertical trends of bacterial limitation by phosphorus and carbon in the Mediterranean Sea, Microbial Ecology 43 (2002) 119–133.

[10] T. F. Thingstad, M. D. Krom, R. F. C. Mantoura, Nature of P limitation in the ultraoligotrophic Eastern Mediterranean, SCIENCE (2005).

[11] T. Tanaka, T. F. Thingstad, U. Christaki, J. Colombet, V. Cornet-Barthaux, C. Courties, J. D. Grattepanche, A. Lagaria, J. Nedoma, L. Oriol, S. Psarra, M. Pujo-Pay, F. Van Wambeke, Lack of P-limitation of phytoplankton and heterotrophic prokaryotes in surface waters of three anticyclonic eddies in the stratified Mediterranean Sea, Biogeosciences 8 (2011) 525–538.

[12] K. Leblanc, J. Arístegui, L. Armand, P. Assmy, B. Beker, A. Bode, E. Breton, V. Cornet, J. Gibson, M.-P. Gosselin, E. Kopczynska, H. Marshall, J. Peloquin, S. Piontkovski, A. J. Poulton, B. Quéguiner, R. Schiebel, R. Shipe, J. Stefels, M. A. van Leeuwe, M. Varela, C. Widdicombe, M. Yallop, A global diatom database – abundance, biovolume and biomass in the world ocean, Earth System Science Data 4 (2012) 149–165.

[13] W. Broecker, T. Peng, Tracers in the Sea. (1982) 1–690.

[14] N. V. D. Broeck, T. Moutin, Phosphate in the sediments of the Gulf of Lions (NW Mediterranean Sea), relationship with input by the river Rhone, Hydrobiologia (2004) 85–94.

[15] W. Ludwig, E. Dumont, M. Meybeck, S. Heussner, River discharges of water and nutrients to the Mediterranean and Black Sea: Major drivers for ecosystem changes during past and future decades?, Progress in Oceanography 80 (2009) 199–217.

[16] J. P. Béthoux, P. Morin, D. P. Ruiz-Pino, Temporal trends in nutrient ratios: Chemical evidence of Mediterranean ecosystem changes driven by human activity, Deep-Sea Research Part II: Topical Studies in Oceanography 49 (2002) 2007–2016.

[17] I. E. Huertas, A. F. Ríos, J. García-Lafuente, G. Navarro, A. Makaoui, A. Snchez-Romn, S. Rodriguez-Galvez, A. Orbi, J. Ruíz, F. F. Pérez,

Atlantic forcing of the Mediterranean oligotrophy, Global Biogeochemical Cycles 26 (2012) 1–9.

[18] K. I. Kopasakis, A. N. Georgoulas, P. B. Angelidis, N. E. Kotsovinos, Simulation of the long term fate of water and pollutants, transported from the Dardanelles plume into the North Aegean Sea, Applied Ocean Research 37 (2012) 145–161.

[19] W. Ludwig, A. F. Bouwman, E. Dumont, F. Lespinas, Water and nutrient fluxes from major Mediterranean and Black Sea rivers: Past and future trends and their implications for the basin-scale budgets, Global Biogeochemical Cycles 24 (2010) 1–14.

[20] D. Macías, A. P. Martin, J. García-Lafuente, C. M. García, A. Yool, M. Bruno, A. Vázquez-Escobar, A. Izquierdo, D. V. Sein, F. Echevarría, Analysis of mixing and biogeochemical effects induced by tides on the Atlantic-Mediterranean flow in the Strait of Gibraltar through a physical-biological coupled model, Progress in Oceanography 74 (2007) 252–272.

[21] H. R. Powley, M. D. Krom, P. Van Cappellen, Understanding the unique biogeochemistry of the Mediterranean Sea: Insights from a coupled phosphorus and nitrogen model, Global Biogeochemical Cycles 31 (2017) 1010–1031.

[22] C. Richon, J. C. Dutay, F. Dulac, R. Wang, Y. Balkanski, P. Nabat, O. Aumont, K. Desboeufs, B. Laurent, C. Guieu, P. Raimbault, J. Beuvier, Modeling the impacts of atmospheric deposition of nitrogen and desert dust-derived phosphorus on nutrients and biological budgets of the Mediterranean Sea, Progress in Oceanography 163 (2018) 21–39.

[23] J.-Y. Moon, K. Lee, T. Tanhua, N. Kress, I.-N. Kim, Temporal nutrient dynamics in the Mediterranean Sea in response to anthropogenic inputs, Geophysical Research Letters (2016) 5243–5251.

[24] M. D. Krom, K.-c. Emeis, P. V. Cappellen, Why is the Eastern Mediterranean phosphorus limited?, Progress in Oceanography 85 (2010) 236–244.

[25] Z. Markaki, M. D. Loÿe-Pilot, K. Violaki, L. Benyahya, N. Mihalopoulos, Variability of atmospheric deposition of dissolved nitrogen and phosphorus in the Mediterranean and possible link to the anomalous seawater N/P ratio, Marine Chemistry 120 (2010) 187–194.

[26] A. Guyennon, M. Baklouti, F. Diaz, J. Palmieri, J. Beuvier, C. Lebaupin-Brossier, T. Arsouze, K. Beranger, J. C. Dutay, T. Moutin, New insights into the organic carbon export in the Mediterranean Sea from 3-D modeling, Biogeosciences 12 (2015) 7025–7046.

[27] C. Ulses, P.-A. Auger, K. Soetaert, P. Marsaleix, F. Diaz, L. Coppola, M. M.J., F. Kessouri, C. Estournel, Budget of organic carbon in the North-Western Mediterranean open sea over the period 2004-2008 using 3-D coupled physical-biogeochemical modeling, Journal of Geophysical Research: Oceans (2016) 1–14.

[28] P. Lazzari, C. Solidoro, S. Salon, G. Bolzon, Spatial variability of phosphate and nitrate in the Mediterranean Sea: A modeling approach, Deep-Sea Research Part I: Oceanographic Research Papers 108 (2016) 39–52.

[29] D. Macias, E. Garcia-gorriz, C. Piroddi, A. Stips, Biogeochemical control of marine productivity in the Mediterranean Sea during the last 50 years, Global Biogeochemical Cycles (2014) 897–907.

[30] H. R. Powley, M. D. Krom, K. C. Emeis, P. Van Cappellen, A biogeochemical model for phosphorus and nitrogen cycling in the Eastern Mediterranean Sea: Part 2: Response of nutrient cycles and primary production to anthropogenic forcing: 1950-2000., Journal of Marine Systems 139 (2014) 420–432.

[31] G. team Madec, NEMO, NEMO ocean engine (2016).

[32] M. Hamon, J. Beuvier, S. Somot, J.-m. Lellouche, E. Greiner, G. Jordà, M.-n. Bouin, T. Arsouze, F. Sevault, M. Hamon, J. Beuvier, S. Somot, J.-m. Lellouche, E. Greiner, M. Hamon, J. Beuvier, S. Somot, J.-m. Lellouche, E. Greiner, G. Jordà, Design and validation of MEDRYS , a Mediterranean Sea reanalysis over the period 1992 – 2013, Ocean Science (2016).

[33] M. Baklouti, V. Faure, L. Pawlowski, A. Sciandra, Investigation and sensitivity analysis of a mechanistic phytoplankton model implemented in a new modular numerical tool (Eco3M) dedicated to biogeochemical modelling, Progress in Oceanography 71 (2006) 34–58.

[34] M. Baklouti, F. Diaz, C. Pinazo, V. Faure, B. Quéguiner, Investigation of mechanistic formulations depicting phytoplankton dynamics for models of marine pelagic ecosystems and description of a new model, Progress in Oceanography 71 (2006) 1–33.

[35] R. Mauriac, T. Moutin, M. Baklouti, Accumulation of DOC in Low Phosphate Low Chlorophyll (LPLC) area : is it related to higher production under high N : P ratio ?, Biogeosciences (2011).

[36] E. Alekseenko, V. Raybaud, B. Espinasse, F. Carlotti, B. Queguiner, B. Thouvenin, P. Garreau, M. Baklouti, Seasonal dynamics and stoichiometry of the planktonic community in the NW Mediterranean Sea: A 3D modeling approach, Ocean Dynamics 64 (2014) 179–207.

[37] A. Gimenez, M. Baklouti, S. Bonnet, T. Moutin, N. Caledonia, Biogeochemical fluxes and fate of diazotroph-derived nitrogen in the food web after a phosphate enrichment: modeling of the VAHINE mesocosms experiment (2016) 5103–5120.

[38] E. Alekseenko, M. Baklouti, F. Carlotti, Main factors favoring Mnemiopsis leidyi individuals growth and population outbreaks : a modelling approach, Journal of Marine Systems (2019).

[39] A. Gimenez, M. Baklouti, T. Wagener, T. Moutin, Diazotrophy as the main driver of the oligotrophy gradient in the western tropical South Pacific Ocean: Results from a one-dimensional biogeochemical-physical coupled model, Biogeosciences 15 (2018).

[40] J. Beuvier, C. L. Brossier, K. Béranger, R. Bourdallé-badie, C. Deltel, Y. Drillet, N. Ferry, F. Lyard, J. Beuvier, C. L. Brossier, K. Béranger, T. Arsouze, R. Bourdallé, MED12, oceanic component for the modeling of the regional Mediterranean earth system. (2012).

[41] M. Fichaut, G. Maria-jesus, G. Alessandra, I. Athanasia, K. Alexander, Achimer MEDAR / MEDATLAS 2002 : A Mediterranean and Black Sea

database for operational oceanography Elsevier Oceanography Series 69 (2003).

[42] E. V. Stanev, J. A. Simeonov, E. L. Peneva, Ventilation of Black Sea pycnocline by the Mediterranean plume, Journal of Marine Systems 31 (2001) 77–97.

[43] J. Palmiéri, J. C. Orr, J.-C. Dutay, K. Béranger, A. Schneider, J. Beuvier, S. Somot, Simulated anthropogenic CO 2 storage and acidification of the, Biogeosciences (2015) 781–802.

[44] A. Guyennon, Etude de l'exportation de carbone organique à l'échelle de la mer Méditerranée à l'aide de la modélisation couplée physique/biogéochimie, Ph.D. thesis, Aix Marseille, 2015.

[45] G. Volpe, R. Santoleri, V. Vellucci, M. Ribera d'Alcalà, S. Marullo, F. D'Ortenzio, The colour of the Mediterranean Sea: Global versus regional bio-optical algorithms evaluation and implication for satellite chlorophyll estimates, Remote Sensing of Environment 107 (2007) 625–638.

[46] L. Coppola, The DYFAMED time series have been provided by the Oceanological Observatory of Villefranche-sur-Mer (L.Coppola). This project is funded by CNRS-INSU and ALLENVI through the MOOSE observing network, 1991.

[47] K. E. Taylor, Summarizing multiple aspects of model performance in a single diagram, Journal of Geophysical Research 106 (2001) 7183–7192.

[48] A. Aminot, R. Kérouel, Dosage automatique des nutriments dans les eaux marines : méthodes en flux continu., Ifremer, 2007.

[49] N. Bahamón, Z. Velásquez, A. Cruzado, Chlorophyll a and nitrogen flux in the tropical North Atlantic Ocean, Deep-Sea Research Part I: Oceanographic Research Papers 50 (2003) 1189–1203.

[50] T. Ozer, I. Gertman, N. Kress, J. Silverman, B. Herut, Interannual thermohaline (1979 – 2014) and nutrient (2002 – 2014) dynamics in the Levantine surface and intermediate water masses , SE Mediterranean Sea, Global and Planetary Change 151 (2017) 60–67.

[51] T. R. Anderson, D. O. Hessen, J. J. Elser, J. Urabe, T. R. Anderson, D. O. Hessen, J. J. Elser, J. Urabe, Metabolic Stoichiometry and the Fate of Excess Carbon and Nutrients in Consumers, American society of naturalists 165 (2005) 1–15.

[52] D. L. Kirchman, Microbial Ecology of the Oceans, Second Edition, 2008.

[53] E. Litchman, Klausmeier, A. Christopher, Trait-Based Community Ecology of Phytoplankton Trait-Based Community Ecology of Phytoplankton, Annual Review of Ecology Evolution and Systematics (2008).

[54] B. Klein, W. Roether, N. Kress, B. B. Manca, M. Ribera, E. Souvermezoglou, A. Theocharis, G. Civitarese, A. Luchetta, Accelerated oxygen consumption in eastern Mediterranean deep waters following the recent changes in thermohaline circulation, Journal of Geophysical Research 108 (2003).

[55] B. Coste, P. L. Corre, H. J. Minas, Re-evaluation of the nutrient exchanges in the strait of gibraltar, Deep Sea Research Part A, Oceanographic Research Papers 35 (1988) 767–775.

[56] R. C. Dugdale, F. P. Wilkerson, V. E. Hogue, A. Marchi, The role of ammonium and nitrate in spring bloom development in San Francisco Bay 73 (2007) 17–29.

[57] J. T. Turner, The importance of small planktonic copepods and their roles in pelagic marine food webs, Zoological Studies 43 (2004) 255–266.

[58] C. Saraux, E. Van Beveren, P. Brosset, Q. Queiros, J. H. Bourdeix, G. Dutto, E. Gasset, C. Jac, S. Bonhommeau, J. M. Fromentin, Small pelagic fish dynamics: A review of mechanisms in the Gulf of Lions, Deep-Sea Research Part II: Topical Studies in Oceanography (2018).

[59] P. Voulgaridou, K. I. Stergiou, Trends in various biological parameters of the European sardine , Sardina pilchardus (Walbaum , 1792), in the Eastern Mediterranean Sea, Scientia Marina 67 (2003) 269–280.

[60] T. Kiorboe, A Mechanistic Approach to Plankton Ecology, Princeton University Press, 2008.